



Cardioprotective O-GlcNAc signaling is elevated in murine female hearts *via* enhanced O-GlcNAc transferase activity

Received for publication, May 24, 2023, and in revised form, October 16, 2023. Published, Papers in Press, November 8, 2023.
<https://doi.org/10.1016/j.jbc.2023.105447>

Bhargavi Narayanan¹, Prithvi Sinha², Roger Henry¹, Russell A. Reeves¹, Nazareno Paolucci^{3,4}, Mark J. Kohr², and Natasha E. Zachara^{1,5,*}

From the ¹The Department of Biological Chemistry at the Johns Hopkins University School of Medicine, Baltimore, Maryland, USA; ²The Department of Environmental Health and Engineering, The Johns Hopkins Bloomberg School of Public Health, Baltimore, Maryland, USA; ³Division of Cardiology, Department of Medicine, Johns Hopkins University School of Medicine, Baltimore, Maryland, USA; ⁴Department of Biomedical Sciences, University of Padova, Padua, Italy; ⁵The Department of Oncology at the Johns Hopkins University School of Medicine, Baltimore, Maryland, USA

Reviewed by members of the JBC Editorial Board. Edited by Robert Haltiwanger

The post-translational modification of intracellular proteins by O-linked β -GlcNAc (O-GlcNAc) has emerged as a critical regulator of cardiac function. Enhanced O-GlcNAcylation activates cytoprotective pathways in cardiac models of ischemia–reperfusion (I/R) injury; however, the mechanisms underpinning O-GlcNAc cycling in response to I/R injury have not been comprehensively assessed. The cycling of O-GlcNAc is regulated by the collective efforts of two enzymes: O-GlcNAc transferase (OGT) and O-GlcNAcase (OGA), which catalyze the addition and hydrolysis of O-GlcNAc, respectively. It has previously been shown that baseline heart physiology and pathophysiology are impacted by sex. Here, we hypothesized that sex differences in molecular signaling may target protein O-GlcNAcylation both basally and in ischemic hearts. To address this question, we subjected male and female WT murine hearts to *ex vivo* ischemia or I/R injury. We assessed hearts for protein O-GlcNAcylation, abundance of OGT, OGA, and glutamine:fructose-6-phosphate aminotransferase (GFAT2), activity of OGT and OGA, and UDP-GlcNAc levels. Our data demonstrate elevated O-GlcNAcylation in female hearts both basally and during ischemia. We show that OGT activity was enhanced in female hearts in all treatments, suggesting a mechanism for these observations. Furthermore, we found that ischemia led to reduced O-GlcNAcylation and OGT-specific activity. Our findings provide a foundation for understanding molecular mechanisms that regulate O-GlcNAcylation in the heart and highlight the importance of sex as a significant factor when assessing key regulatory events that control O-GlcNAc cycling. These data suggest the intriguing possibility that elevated O-GlcNAcylation in females contributes to reduced ischemic susceptibility.

Cardiovascular disease (CVD), including ischemia–reperfusion (I/R) injury, is impacted by both sex and gender. Sex refers to biological attributes encoded by DNA (*e.g.*, reproductive organs), whereas gender is multidimensional and relates to social and cultural behaviors (1). While gender impacts access to health care and implementation of prevention, sex affects disease presentation, pathophysiology, and treatment response. The prevalence of myocardial infarction (MI; I/R injury) was 4.5% for males and 2.1% for females (>20 years of age) from 2017 to 2020 (2). The risk of MI rises sharply in female's postmenopause and in young women who have had an oophorectomy (3–5). In rodent studies, females exhibit enhanced recovery and smaller infarcts compared with males and ovariectomized females (6–9). Loss of cardioprotection in the aforementioned models has been attributed to a decline in estrogen, namely 17 β -estradiol. Reinforcing this hypothesis are data from rodents where treatment with 17 β -estradiol, or agonists of estrogen receptors, reduces infarct size and fibrosis while improving heart function (8, 10, 11). However, clinical outcomes have not supported a cardioprotective role for estrogen(s). For instance, hormone replacement therapy–based clinical trials failed to exhibit a reduction in heart disease following hormone administration. In fact, some trials exhibited an increased risk of CVD events suggesting a more complicated picture than simply replacing estrogen (12). These inconsistent findings highlight the importance of examining baseline biological differences between male and female hearts that will help elucidate the influence of both components of biological sex (gonadal hormones and genetics) on heart function basally and in response to injury. While molecular processes that regulate cardiac physiology such as protein S-nitrosylation (SNO) have been studied in male and female hearts (6, 13), to date, the impact of sex on cardioprotective signaling mediated by protein O-GlcNAcylation has not been assessed.

O-linked β -O-GlcNAc, is an essential and dynamic post-translational modification of more than 5000 nuclear, mitochondrial, and cytosolic proteins (14–16). O-GlcNAc modification, or O-GlcNAcylation, of proteins impacts their function and in turn diverse cellular processes that include

* For correspondence: Natasha E. Zachara, nzachara@jhmi.edu.

Present addresses for: Prithvi Sinha, Perelman Center for Advanced Medicine, University of Pennsylvania, Philadelphia, Pennsylvania, USA; Roger Henry, Department of Ophthalmology and Visual Sciences at the Rutgers University New Jersey Medical School Newark, New Jersey, USA; Russell A. Reeves, Department of Radiology, Sidney Kimmel Medical College at Thomas Jefferson University, Philadelphia, Pennsylvania, USA.

Sex differences in O-GlcNAc cycling in the heart

proteostasis, metabolism, signal transduction, mitochondrial function, epigenetics, and transcriptional regulation (17–21). The dynamic cycling of protein O-GlcNAcylation is regulated by two enzymes: the O-GlcNAc transferase (OGT) and the O-GlcNAcase (OGA) that catalyze the addition and removal of O-GlcNAc, respectively (22–24). OGT uses the nucleotide sugar UDP-GlcNAc, which is synthesized by the hexosamine biosynthetic pathway (HBP). The rate-limiting enzyme of the HBP is the glutamine-fructose 6 phosphate amidotransferase (GFAT) (14, 15). Demonstrating the importance of O-GlcNAcylation in both cell function and physiology, deletion of OGT or OGA in mammals is lethal (25–27).

A rapid, dynamic, and global elevation of O-GlcNAcylation is observed in response to environmental stressors (*e.g.*, heat shock, oxidative, osmotic) as well as physiological models of tissue injury (*e.g.*, ischemic preconditioning [IPC]) (28–36). Enhancing O-GlcNAc levels in cells before heat stress promotes survival and the induction of heat shock proteins—suggesting that stress-induced cycling of O-GlcNAc leads to cytoprotection (28, 29). Critically, the cytoprotective role of O-GlcNAc is not restricted to cellular models, with several groups demonstrating that acute increases in protein O-GlcNAcylation are cardioprotective (34–43). For instance, elevating O-GlcNAc levels prior to ischemia or during reperfusion significantly improves heart function (*ex vivo*) and reduces infarct size (*in vivo*) (33–37, 39). In contrast, inducible deletion of OGT prior to I/R injury (*in vivo*) results in a significant decline in left ventricular function and increased cardiac fibrosis and cardiomyocyte death (44). Supporting a cytoprotective role of O-GlcNAc in the heart, elevating O-GlcNAc levels in cardiac models suppresses all the hallmarks of I/R injury, including reducing reactive oxygen species release and endoplasmic reticulum stress, preserving mitochondrial membrane potential, inhibiting opening of the mitochondrial permeability transition pore, and preventing

calcium overload (37, 42, 45–47). Despite its well-documented role in cardioprotection and CVD, the mechanisms regulating O-GlcNAc cycling in the heart are ill defined.

To address these gaps in knowledge, we have compared O-GlcNAc cycling in male and female hearts subjected to control, ischemic, and I/R injury *ex vivo*, using methodology that enables measurement of enzymatic activity, protein abundance (OGT, OGA, and GFAT2), and UDP-GlcNAc levels from a single heart. In ischemic samples, lower levels of O-GlcNAc were detected, and this was associated with a reduction in OGT activity. Notably, we observed elevated O-GlcNAcylation in female hearts before and after injury, which was associated with enhanced OGT activity. Collectively, our data and that of others underpin the importance of examining sex differences with the intact influence of hormones on fundamental biochemical signaling pathways that impact cardiac homeostasis and disease.

Results

O-GlcNAc levels are enhanced in female hearts compared with age-matched male hearts

Motivating our interest in assessing the impact of sex on O-GlcNAcylation are reports demonstrating that *Ogt* is X-linked, that male embryos have lower levels of O-GlcNAc than females in a placental stress model, and that in hearts subjected to transverse aortic constriction (TAC)—OGT abundance is transiently higher in female hearts than in males (27, 48, 49). To characterize O-GlcNAc cycling in male and female murine hearts basally, we assessed the levels of O-GlcNAc as well as the abundance of OGT, OGA, and GFAT2 in total tissue lysates (9 M urea, N = 5/sex) using immunoblotting. We used the RL2 antibody to detect O-GlcNAc, as we have previously shown that this detects cardiac contractile proteins with greater sensitivity than CTD110.6 (50). The data presented in Figure 1 demonstrate elevated O-GlcNAc levels (~35%) in female hearts

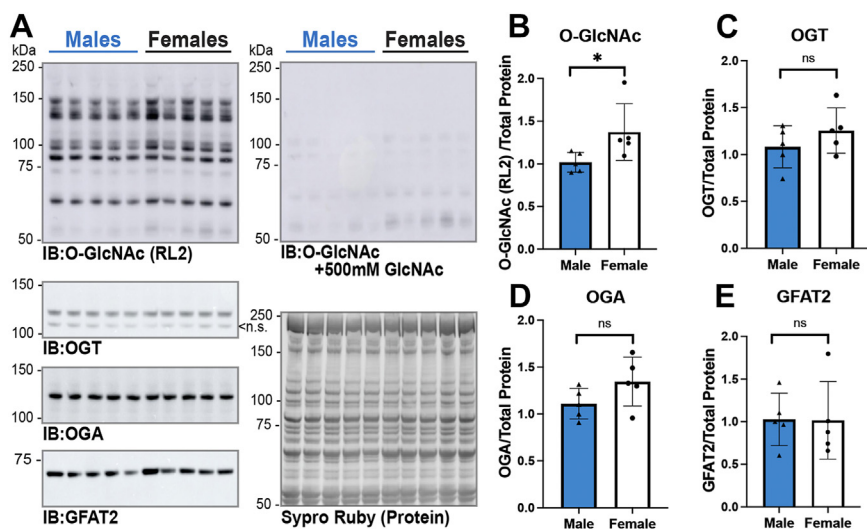


Figure 1. O-GlcNAc levels are enhanced in female hearts compared with age-matched male hearts. A, total tissue lysates of hearts from C57B6/J WT mice (14–18 weeks, N = 5 per sex) were generated using 9 M urea. Proteins were separated by SDS-PAGE (15 or 22.5 μ g), electroblotted to nitrocellulose, and the following were detected and quantified: O-GlcNAc (RL2), O-GlcNAc specificity control (RL2 with 500 mM GlcNAc), O-GlcNAc transferase (OGT), O-GlcNAcase (OGA), and glutamine fructose-6-phosphate amidotransferase 2 (GFAT2). Protein load was assessed by total protein membrane stain (SYPRO Ruby). The following signals were quantified and normalized to total protein (B) O-GlcNAc (RL2); (C) OGT; (D) OGA; and (E) GFAT2. Statistical test: unpaired Student's *t* test. **p* < 0.05. B–E, data are represented as mean \pm SD. ns, nonspecific band; O-GlcNAc, O-linked β -GlcNAc.

compared with age-matched male hearts. As a control, the O-GlcNAc antibody RL2 was competed away with free GlcNAc. The residual signal is due to endogenous immunoglobulin (immunoglobulin G [IgG] heavy chain ~55 kDa) and has not been included in the quantitation. No significant change in the abundance of OGT, OGA, or GFAT2 was detected. GFAT2 has been reported as the primary myocardial variant of GFAT, and consistent with this report, we were unable to detect GFAT1 in murine heart lysates (*data not shown*). Of note, anti-OGT (O6264; MilliporeSigma) detected two OGT bands; one of which has a similar migration to the mitochondrial isoform of OGT. However, this band was not detected using two antibodies (O6139 and O6014; MilliporeSigma) with independent epitopes (amino acids 833–849 [O6139]; 1024 to 1037 [O6014]; OGT numbering: UniProtKB: O15294-1) present in both full-length and mitochondrial OGT isoforms (*data not shown*). Thus, we conclude that this band is nonspecific. Together, these data demonstrate that elevated levels of O-GlcNAc in female hearts do not arise from changes in the abundance of the O-GlcNAc cycling enzymes (OGT/OGA) or the rate-limiting enzyme of the HBP (GFAT2).

Female hearts begin ischemic contracture and reach hypercontracture earlier than age-matched male hearts

Prior experiments have demonstrated dynamic changes in O-GlcNAcylation in response to ischemia and I/R injury

(32–34, 37, 51). In an *ex vivo* perfusion model in rats, O-GlcNAcylation increases after 10 min of ischemia but declines between 10 and 30 min of ischemia and remains depressed at 60 min of reperfusion (34). To assess the impact of ischemia and I/R injury in mice, we used the Langendorff perfused heart model to collect hearts exposed to either 20 min of ischemia or ischemia with 40 to 120 min of reperfusion. Consistent with data in rat hearts, our pilot studies demonstrate a reduction in O-GlcNAc (CTD110.6) on soluble heart proteins at 20 min of ischemia in male hearts (Fig. S1A). We assessed O-GlcNAc at 40, 80, and 120 min of reperfusion, determining that O-GlcNAcylation remains low at 40 and 80 min, before rebounding at 120 min (Fig. S1B).

To determine if sex impacts O-GlcNAcylation and heart function during ischemia and reperfusion, we collected a cohort of murine male and female hearts exposed to 20 min of ischemia (ischemia) or 20 min of ischemia and 120 min of reperfusion (I/R) *ex vivo* on the Langendorff apparatus (Fig. 2A). A representative left ventricular developed pressure (LVDP) trace is presented (Fig. 2B). Consistent with prior data, our measurements indicated no differences in LVDP and heart rate (HR) between male and female hearts (Fig. 2C) (13). Using the pressure traces, we also assessed time in ischemic contracture between male and female hearts (Fig. 2, B and D). While no difference in the duration of contracture was observed, we detected a sex-dependent difference in the initiation of contracture and the time to hypercontracture

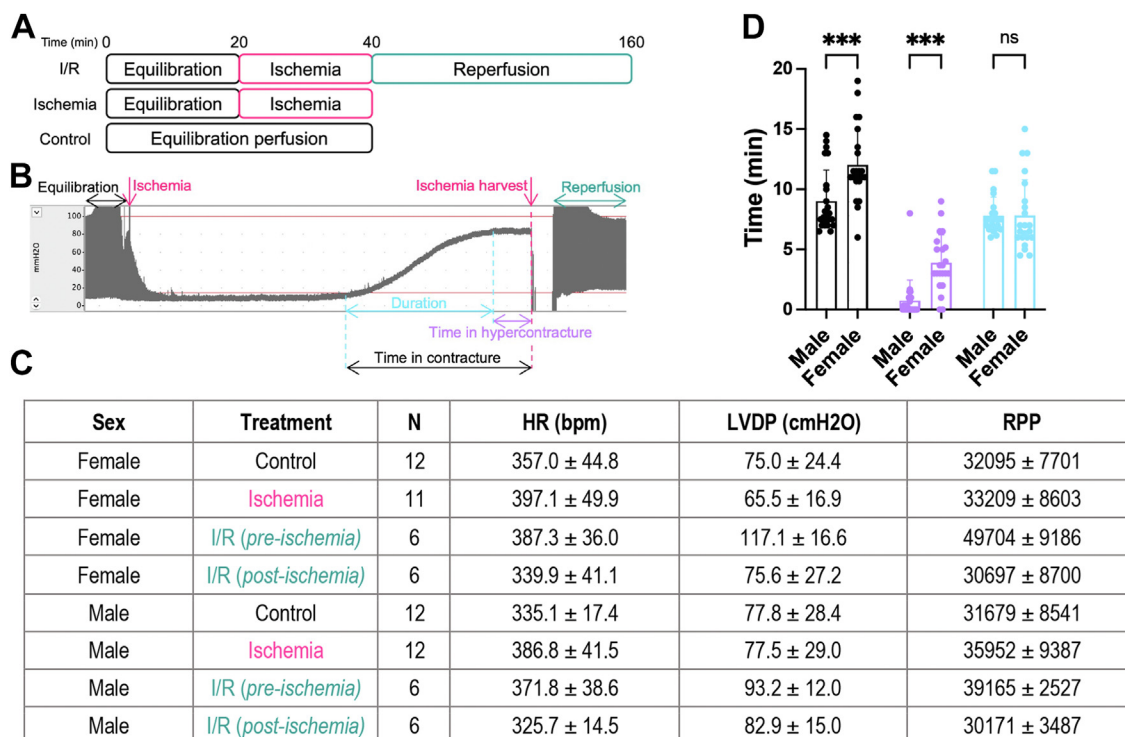


Figure 2. Female hearts begin ischemic contracture and reach hypercontracture earlier than age-matched male hearts. Hearts from C57B6/J WT mice (15–21 weeks, N = 6–12 per sex per treatment) were treated *ex vivo* on the Langendorff apparatus. A, perfusion protocol: control—40 min perfusion; ischemia—20 min perfusion, 20 min—no-flow ischemia; ischemia-reperfusion (I/R) injury—20 min ischemia, 120 min reperfusion. B, representative I/R left ventricular developed pressure (LVDP) trace obtained during perfusion. Critical time points are highlighted. C, summary of pre-ischemic and postischemic contractile parameters. Heart rate (HR), LVDP, and rate pressure product (RPP) were recorded for all replicates and represented as mean ± SD. D, comparison of time in contracture (●), time in hypercontracture (●), and the duration of contracture (●) between males and females. Statistical test: two-way ANOVA. ****p* < 0.001. Data are represented as mean ± SD.

Sex differences in O-GlcNAc cycling in the heart

(Fig. 2D). Female hearts begin to go into contracture and reach hypercontracture faster than male counterparts, possibly as these hearts contain less glycogen content and exhaust energy reserves faster than male hearts (52).

O-GlcNAc levels cycle in response to I/R injury with little impact on OGT and OGA abundance

To assess O-GlcNAc cycling in injured hearts, we measured O-GlcNAc levels, the abundance of OGT, OGA, and GFAT2, OGT and OGA activity, and UDP-GlcNAc levels. O-GlcNAcylation in the aforementioned hearts was determined in total tissue lysates (1% NP-40) by immunoblotting using the RL2 antibody (Fig. 3A). Quantitation of O-GlcNAc immunoblots demonstrated a modest decrease in O-GlcNAcylation after 20 min of ischemia in both male and female hearts (Fig. 3, A and B). After 120 min of reperfusion, O-GlcNAcylation returns to baseline. Like the data presented in Figure 1B, elevated O-GlcNAcylation (~30%) was detected in female hearts. This observation is especially evident in control and ischemic hearts (Fig. 3, A and B).

Prior studies have correlated changes in O-GlcNAc with the abundance of the enzymes that cycle O-GlcNAc (OGT and OGA) or are critical to UDP-GlcNAc synthesis (GFAT2) in models of I/R injury, IPC, and remote ischemic preconditioning (rIPC) (32, 33, 51). Thus, we assessed OGT, OGA, and GFAT2 abundance in these hearts (Fig. 3, C–E). We observed no significant injury-induced changes in the

abundance of OGT (Fig. 3C), OGA (Fig. 3D), and GFAT2 (Fig. 3E). However, like O-GlcNAc levels, we observed elevated GFAT2 abundance in female hearts compared with males (Fig. 3E). This observation is unlike our prior data in Figure 1E and appears to be driven by a modest elevation in GFAT2 in ischemic female hearts.

OGT activity is elevated in female hearts

To provide insight into the mechanisms underpinning sex- and injury-dependent changes in O-GlcNAcylation, we assessed the activity of OGT and OGA in total heart lysates (1% NP-40) using pseudosubstrates as we have previously reported (53–55). We observed a significant reduction in OGT-specific activity (~25%) after 20 min of ischemia (Fig. 4A) that rebounds during reperfusion. A similar pattern in OGT activity is observed in both males (27%) and females (24%) during ischemia and I/R injury; however, there is a strong sex-dependent impact on OGT activity with female hearts displaying higher OGT activity (~20%) compared with age-matched male hearts (Fig. 4A). While OGA activity appears unaffected by injury in males, ischemia elevates OGA activity in female hearts (27%) (Fig. 4B). OGT and OGA activity mirror our pilot studies (Fig. S1), which used soluble lysates from male hearts. As OGT activity and O-GlcNAc showed a similar trend basally and in response to injury in both males and females, we performed a correlation analysis of O-GlcNAc to OGT and OGA activity. While O-GlcNAc did not correlate

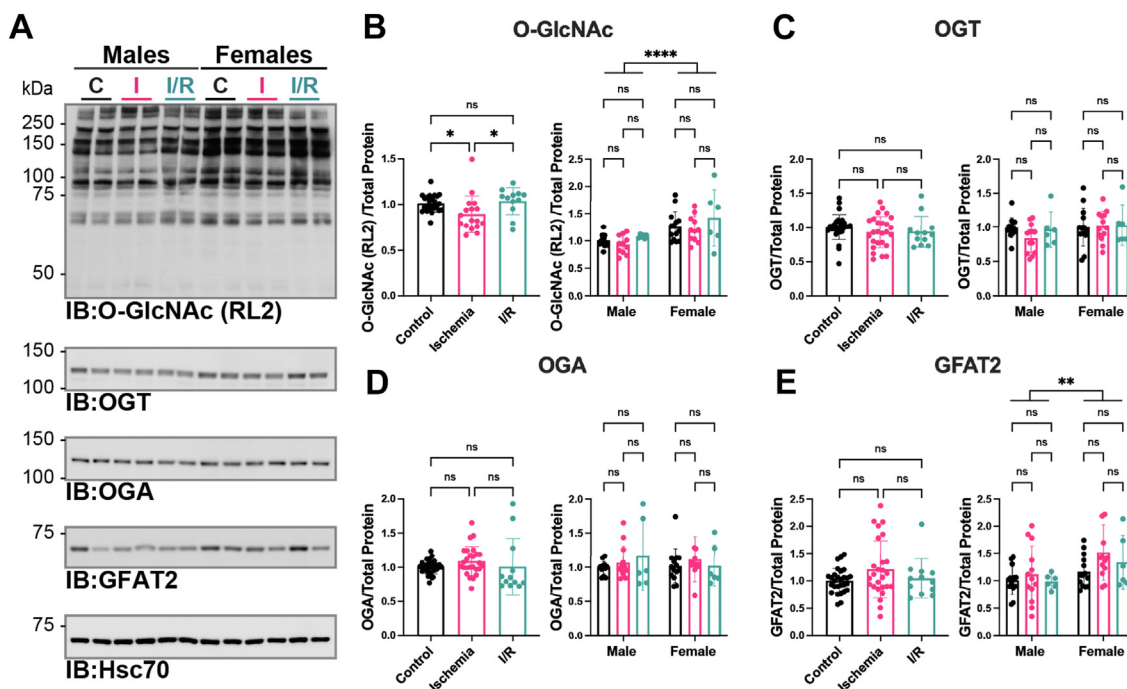


Figure 3. O-GlcNAc levels cycle in response to I/R injury with little impact on OGT and OGA abundance. A, hearts from C57B6/J WT mice (15–21 weeks, N = 6–12 per sex per treatment) were perfused *ex vivo* on the Langendorff apparatus (control [●]; ischemia 20 min [●]; I/R 20 min ischemia/120 min reperfusion [●]). Hearts were extracted in 1% N-P40 buffer, and proteins were separated by SDS-PAGE (15 or 22.5 μg), electroblotted to nitrocellulose, and the following were detected: OGT, OGA, GFAT2, heat shock cognate 70 (Hsc70), O-GlcNAc (RL2), and O-GlcNAc specificity control (RL2 with 500 mM GlcNAc, not shown). Hsc70 was used as a representative immunoblot for protein load. Protein load was assessed by total protein membrane stain (SYPRO Ruby or Direct Blue-71, Fig. S2). The following were quantified and normalized to total protein. (B) O-GlcNAc (RL2); (C) OGT; (D) OGA; and (E) GFAT2. B–E, pooled male and female data are reported on the left. Statistical test: one-way ANOVA. **p* < 0.05. Data parsed by sex are reported on the right. Statistical test: two-way ANOVA. ***p* < 0.01; *****p* < 0.0001. Data are represented as mean ± SD. GFAT2, glutamine-fructose 6 phosphate amidotransferase 2; IR, I/R, ischemia-reperfusion; OGA, O-GlcNAcase; O-GlcNAc, O-linked β-GlcNAc; OGT, O-GlcNAc transferase.

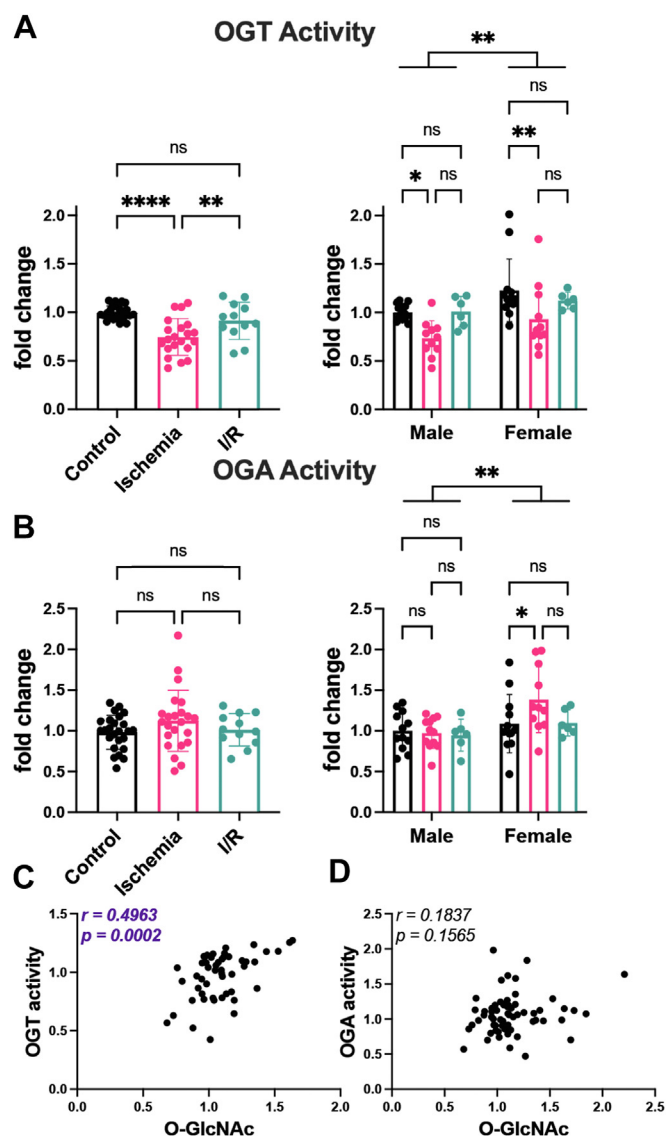


Figure 4. OGT activity is elevated in female hearts. Hearts from C57B6/J WT mice (15–21 weeks, N = 6–12 per sex per treatment) were perfused *ex vivo* on the Langendorff apparatus (control [●]; ischemia 20 min [●]; I/R 20 min ischemia/120 min reperfusion [●]). Hearts were extracted in 1% NP-40, and equal protein was desalted using a Zebaspin column. *A*, OGT activity was assessed by measuring transfer of ^3H -GlcNAc to the casein kinase II (CK2) acceptor peptide. *B*, OGA activity was detected using the pseudo-substrate 4-methylumbelliferyl- β -GlcNAc. *A* and *B*, pooled male and female data are reported on the *left*. Statistical test: one-way ANOVA. **** $p < 0.01$; **** $p < 0.0001$. Data parsed by sex are reported on the *right*. Statistical test: two-way ANOVA. * $p < 0.05$; ** $p < 0.01$. Data are represented as mean \pm SD. *C*, correlation of OGT activity and O-GlcNAc (RL2). *D*, correlation of OGA activity and O-GlcNAc (RL2). *C* and *D*, r = Pearson correlation coefficient. I/R, ischemia–reperfusion; OGA, O-GlcNAcase; OGT, O-GlcNAc transferase.

with OGA activity, O-GlcNAc and OGT activity showed a positive correlation (Fig. 4, C and D). Collectively, these data suggest that sex-dependent and injury-induced changes to O-GlcNAcylation are driven by changes in OGT activity.

UDP-GlcNAc levels do not change during injury in male or female hearts

Prior studies have indicated that activation of X-box binding protein 1 (Xbp1) by ischemic injury leads to changes in

GFAT1 abundance and in turn UDP-GlcNAc levels albeit at latter time points (24 h of reperfusion) (51). As Xbp1 can also be activated by 17- β -estradiol, we assessed UDP-GlcNAc levels in male and female hearts (56). Here, we used a modified Folch extraction to isolate nucleotide sugars, followed by solid phase cleanup, and detection and analysis *via* ion exchange chromatography. We did not observe any sex- or injury-dependent changes to UDP-GlcNAc levels (Fig. 5, A and B). We note that one previous study in an *ex vivo* perfused rat model of I/R injury detected an elevation of UDP-HexNAc during ischemia that returned to baseline during reperfusion (34). As the method used to detect UDP-GlcNAc was similar, the inconsistency in the UDP-GlcNAc levels between our studies likely results from the method used to normalize nucleotide sugar levels in the heart. We normalized UDP-GlcNAc to total protein instead of wet tissue weight. We chose this approach as ischemic hearts appeared smaller than their counterparts; however, ischemic hearts consistently yielded higher protein (protein yield/wet weight) than control or I/R hearts (Fig. S3A). To address the hypothesis that the difference between our observation and those of Fülöp *et al.* arose from differences in normalization technique, we represented our data as UDP-GlcNAc normalized to wet tissue weight (Fig. S3B). These data demonstrate an elevation in UDP-GlcNAc during ischemia that returns to baseline during reperfusion. Collectively, these data suggest that normalizing nucleotide sugars to total protein will yield a more accurate assessment of nucleotide sugar levels. In agreement with this conclusion, Olson *et al.* (57) also normalized nucleotide sugars to total protein to avoid variation from including perfusion buffer. While our studies initially solubilized proteins in 1% w/v SDS; further refinement of our approach demonstrates that hydrolyzing the protein in 0.1 M aqueous NaOH results in \sim 10% more protein than SDS alone. In future studies, we would suggest directly solubilizing proteins in 0.1 M aqueous NaOH.

In parallel with assessing UDP-GlcNAc, we assessed ATP, ADP, and AMP abundance (Fig. 5, C–E). While we did not observe any impact of sex on the levels of adenine nucleotides in the heart, as expected, we detected significant changes during injury. After 20 min of ischemia, we detected a 70% decrease in ATP, a 35% decrease in ADP, and a 30% increase in AMP. In contrast, during reperfusion, AMP and ADP levels are depressed, whereas ATP levels return to baseline (Fig. 5, C–E). Previous data suggest that altered flux through the HBP impacts O-GlcNAc levels; however, we observed no correlation between O-GlcNAc and UDP-GlcNAc levels (Fig. 5F). In contrast, we observed a negative correlation between the AMP:ATP ratio and OGT activity (Fig. 5G) suggesting that as AMP levels rise, OGT activity is depressed.

Discussion

O-GlcNAcylation is a critical regulator of cardiac function (40, 43). Prolonged elevation of O-GlcNAc is associated with hypertension, heart failure (pressure overload), and diabetic cardiomyopathy (58–60). In contrast, IPC and rIPC lead to

Sex differences in O-GlcNAc cycling in the heart

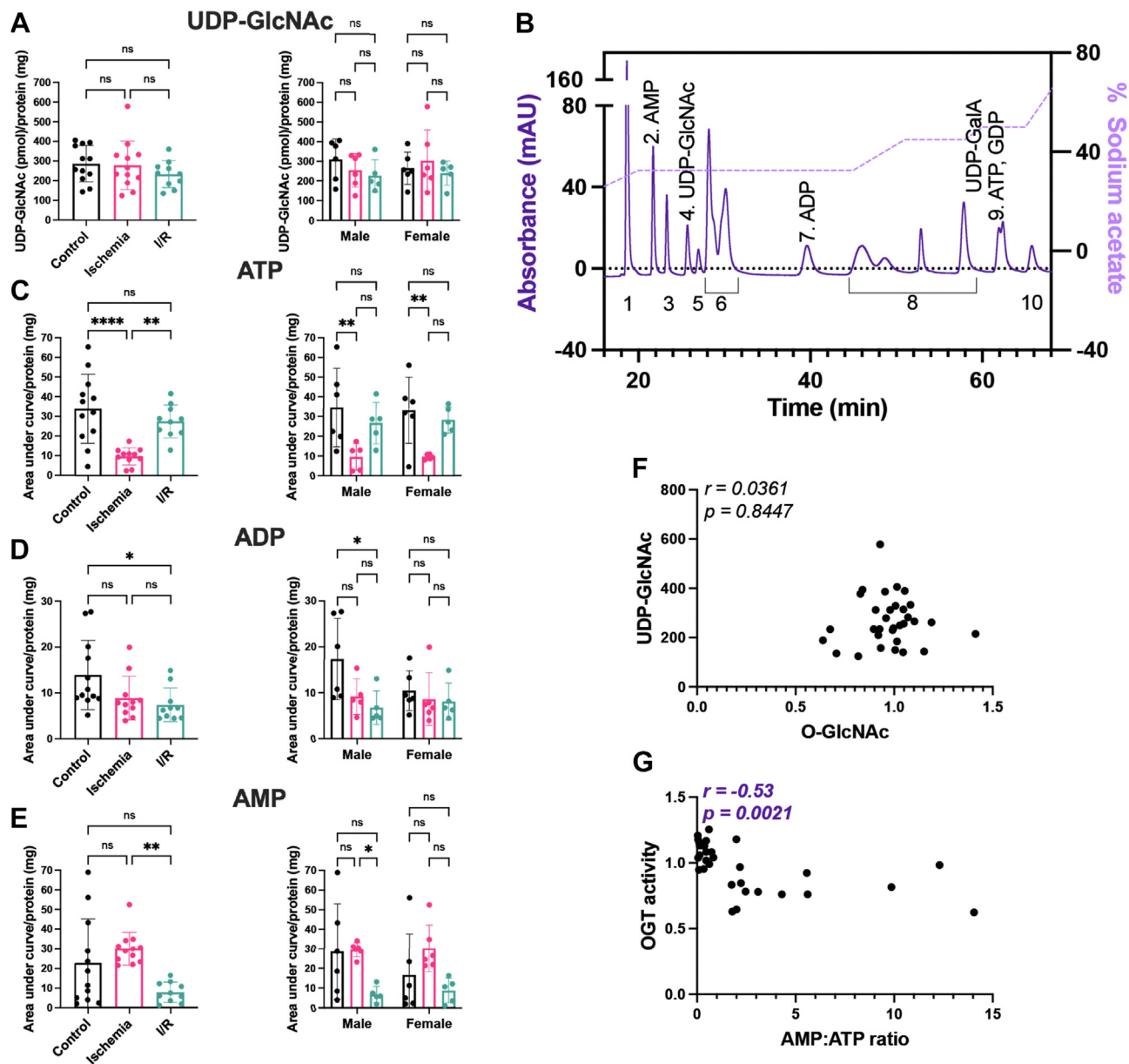


Figure 5. UDP-GlcNAc levels do not change during injury in both male and female hearts. Hearts from C57B6/J WT mice (15–21 weeks, N = 5–6 per sex per treatment) were perfused *ex vivo* on the Langendorff apparatus (control [●]; ischemia 20 min [●]; I/R 20 min ischemia/120 min reperfusion [●]). Heart nucleotides and nucleotide sugars were extracted in methanol:chloroform, desalted using solid-phase extraction, and analyzed using high-performance anion-exchange chromatography. Nucleotide/nucleotide sugar levels were normalized to total protein: (A) UDP-GlcNAc; (B) ATP; (C) ADP; (D) AMP. A–D, pooled male and female data are reported on the left. Statistical test: one-way ANOVA. * $p < 0.05$; ** $p < 0.01$; and **** $p < 0.0001$. Data parsed by sex are reported on the right. Statistical test: two-way ANOVA. * $p < 0.05$; ** $p < 0.01$. Data are represented as mean \pm SD. E, representative separation of nucleotide sugars. Peaks are numbered as follows: (1) CMP, CMP-neuraminic acid; (2) AMP; (3) UMP; (4) UDP-GlcNAc; (5) UDP-GalNAc; (6) UDP-glucose, UDP-galactose, UDP-xylose, CDP, GMP; (7) ADP; (8) UDP, GDP-mannose, GDP-fucose, CTP, UTP; (9) ATP, GDP; and (10) UDP-glucuronic acid. The sodium acetate gradient used to achieve nucleotide separation is depicted on the right Y-axis. F, correlation of UDP-GlcNAc and O-GlcNAc (RL2). G, correlation of AMP:ATP ratio and OGT activity. F and G, r = Pearson's correlation coefficient. I/R, ischemia–reperfusion.

elevated levels of O-GlcNAc, and augmenting O-GlcNAc transiently is cardioprotective in both *ex vivo* and *in vivo* models of cardiac I/R injury (32–34, 36–38, 61). However, the molecular mechanisms by which the heart regulates O-GlcNAcylation are not well understood. In the present study, we document that female hearts have elevated O-GlcNAcylation both basally and during ischemia. As discussed in more detail later, changes in OGT activity drive both sex- and injury-dependent changes in O-GlcNAcylation.

Elevated O-GlcNAc and OGT activity in female hearts

Our study has identified significantly elevated O-GlcNAcylation in female hearts both basally and in models of ischemia and I/R injury (Figs. 1B and 3B). While we did not observe any change in the abundance of OGT, OGA, and GFAT2, or UDP-GlcNAc levels, the specific activity of OGT was elevated in female hearts (Fig. 4A). *Ogt* is X-linked; however, as protein abundance did not change, these data suggest that sex-dependent signaling regulates the activity of OGT. Our

observations are unlike previous data in a murine model of pressure overload-induced cardiac hypertrophy (TAC), where Zhu *et al.* (48) demonstrated no basal differences in cardiac O-GlcNAcylation between males and females. The discrepancy in our datasets can be explained by differences in the O-GlcNAc detection technique. Zhu *et al.* (48) used either RL2 or CTD110.6 to detect O-GlcNAc. In contrast, we used RL2. Our recent studies demonstrate that CTD110.6 has a strong preference for soluble proteins, whereas RL2 will detect both soluble and contractile proteins of the heart (50). Suggesting that females have an enhanced rate of O-GlcNAc cycling compared with males, we also detected elevated OGA activity in females exposed to ischemia (Fig. 4B). These data echo studies focused on the cardioprotective role of nitric oxide (NO) and SNO. Female hearts display elevated NO synthase and protein SNO compared with males (6). Counterintuitively, females exhibited higher activity of the enzyme that mediates SNO catabolism, S-nitrosoglutathione reductase. Notably, loss of S-nitrosoglutathione reductase activity promotes protection in male hearts but exacerbates I/R injury in females (13).

The heart is not the only model in which sex-dependent O-GlcNAcylation has been studied. Huynh *et al.* (62) demonstrated that inhibition of OGA differentially associated with sex-dependent changes in mitochondrial parameters as well as the abundance of autophagy-related and neurodegenerative disease-related proteins. However, no difference in O-GlcNAcylation, OGT and OGA abundance, and OGA activity was detected between males and females. In contrast, in the uterus, elevated levels of OGT and O-GlcNAc are detected in the placenta of female embryos when compared with that of males (49). These data suggest that OGT activity and abundance is regulated by different mechanisms in different tissues and/or different times of development. Reinforcing this supposition are data describing the differential regulation of *Ogt* and *Oga* mRNA maturation in cancer models and a murine model in which OGA activity has been ablated. *Ogt* and *Oga* mRNA maturation is controlled by detained intron splicing that in turn responds to cellular O-GlcNAcylation. Thus, when O-GlcNAc levels are high—maturation of *Ogt* mRNA is inhibited and *Oga* mRNA is favored (63). In some cancer models, this regulation appears to be lost, and, as a result, high O-GlcNAc, OGT, and HBP enzyme abundance are observed (64–66). Similarly, in murine embryos, loss of OGA catalytic activity showed tissue-specific regulation of *Ogt* and *Oga* mRNA abundance and maturation (67). While elevated O-GlcNAcylation and OGA protein abundance were observed in the brain and liver, enhanced maturation of *Oga* mRNA occurred only in the liver, whereas mature *Oga* mRNA levels in the brain remained unchanged. Conversely, mature *Ogt* mRNA levels and protein abundance were found to be reduced only in the brain (67).

OGT activity and O-GlcNAc are depressed during ischemia

Several studies have reported dynamic cycling of O-GlcNAcylation in the heart during injury. In agreement with prior studies (34), we demonstrate a reduction in O-GlcNAc

during ischemia, which rebounds during reperfusion (Figs. S1 and 3B). This phenotype is more pronounced in soluble heart lysates (Fig. S1); however, as a significant proportion of the OGT remains associated with the contractile fraction using this lysis method, enzyme assays used total tissue lysates (50). To begin to understand the mechanisms regulating O-GlcNAc cycling, we examined the abundance of the O-GlcNAc-cycling enzymes (OGT, OGA, and GFAT2), OGT and OGA activity, and UDP-GlcNAc levels in hearts, either after 20 min of ischemia or after 120 min of reperfusion. While we do not observe changes in the abundance of OGT, our studies revealed a significant decrease in OGT activity (25%) during ischemia that rebounds during reperfusion (Figs. 3, 4A, and S1A). Prior studies highlight the physiological significance of modest changes in O-GlcNAcylation. For instance, increased O-GlcNAcylation (20%) in the adipose and muscle of mice results in insulin resistance and hyperleptinemia (68). In the murine heart, adenoviral overexpression of OGT results in a 20% increase in O-GlcNAcylation, as well as cardiac remodeling and dysfunction, increased reactive oxygen species, and altered phosphoinositide 3-kinase signaling (69). Finally, in an inducible cardiomyocyte knockout of OGT, left ventricular dysfunction was exacerbated post-MI; however, O-GlcNAcylation was only depressed by 20% (70).

During ischemia, contractile force declines within 10 s and is abolished within a few minutes. After 10 to 20 min, diastolic tension gradually rises, and ischemic contracture occurs (Fig. 2B). While the exact mechanisms underlying contracture are unknown, several studies suggest that the rise in resting tension is mediated by the formation of rigor bridges because of low ATP concentration at myofilaments and changes in cellular Ca^{2+} homeostasis. From our LVDP measurements, we observed that female hearts begin to go into contracture and reach a hypercontracted state faster than male hearts. Consequently, female hearts were in hypercontracture longer at the time of harvest. A similar observation was made by Penna *et al.* (71) using an *ex vivo* perfusion of rat hearts. As female hearts have higher O-GlcNAc basally and during injury, we performed a correlation analysis that showed no positive correlation between O-GlcNAc and time in contracture/hypercontracture (Fig. S4, A and B). Similarly, no correlation was detected between time in contracture or hypercontracture and OGT activity (Fig. S4, C and D). We did detect a negative correlation between the AMP:ATP ratio and OGT activity consistent with a reduction in OGT activity during ischemia (Fig. 5G). OGT is regulated by kinases that respond to energy balance, such as AMP-activated protein kinase (72, 73) and glycogen synthase kinase 3 β (GSK3 β) (74). AMP-activated protein kinase activates OGT in a model of glucose deprivation in skeletal muscle myotubes resulting in the increased O-GlcNAcylation of nuclear proteins (73). GSK3 β phosphorylates and activates OGT from murine brain extracts (74). Alternatively, Chang *et al.* (75) demonstrated that activation of PKA by forskolin in a model of glucose deprivation decreased O-GlcNAcylation in rat kidney cells. Our data would be consistent with reduced GSK3 β and/or enhanced PKA signaling that have been reported during ischemia (76–78).

Sex differences in O-GlcNAc cycling in the heart

As previous studies have implicated HBP flux in regulating O-GlcNAc levels in models of I/R injury (34, 51), our studies addressed the abundance of GFAT2—the rate-limiting enzyme of the HBP. We note that prior studies have demonstrated that both GFAT1 and GFAT2 are expressed in the myocardium; however, GFAT2 is both the more abundant isoform and the primary regulator of cardiac O-GlcNAcylation (79). In agreement with these observations, we were unable to detect GFAT1. We observed little change in GFAT2 abundance, except for female hearts subjected to ischemia (Fig. 3E). Nonetheless, we did not detect any changes to UDP-GlcNAc during injury in both males and females (Fig. 5A). In a recent study, Olson *et al.* (57) assessed glucose flux through the HBP in an *ex vivo* perfused heart by radiolabeling followed by LC-MS. They demonstrated that reducing cardiac workload by arresting ventricular contractions did not impact HBP flux, and UDP-GlcNAc remained stable from 20 to 40 min of perfusion. These observations agree with our data where we observed no changes to UDP-GlcNAc levels after 20 min of ischemia or after 120 min of reperfusion. Collectively, as no change in UDP-GlcNAc levels were detected, these data suggest that alterations in OGT activity are the major driver of changes in O-GlcNAcylation in the heart and that during early time points in reperfusion, cellular UDP-GlcNAc pools and HBP flux are sufficient to supply OGT.

The role of HBP and protein O-GlcNAcylation on cardiovascular function is well established. Several groups have demonstrated that acute changes in O-GlcNAcylation are cardioprotective, whereas prolonged enhancement or depression promotes heart failure (32–39, 44, 61, 69, 80–88). Recent studies have highlighted some mechanisms underlying changes in O-GlcNAcylation during acute stress such as IPC and rIPC and in more chronic settings, such as diabetes, hypertension, cardiac hypertrophy, and MI. In murine and rat pressure overload-induced hypertrophy (TAC) models, elevated O-GlcNAcylation (12–60%) was associated with increased abundance of OGT (20–150%) and GFAT2 (10%). The impact of TAC on OGA abundance is mixed, with both an increase (300%) and decrease (–40%) observed (44, 58, 88). In an MI-induced heart failure model, increased O-GlcNAcylation (60%) was associated with lower abundance of OGA (25%), increased abundance of OGT (110%), and upregulation of miRNA-539 (89). While OGT and OGA activity have not been examined during heart failure, in models such as IPC and rIPC, elevated O-GlcNAcylation (50%) is associated with increased OGT abundance (100%) and activity (100–300%) (32, 33). These data are consistent with our data where changes in O-GlcNAcylation are driven by changes in OGT activity. We posit that transient cycling of O-GlcNAcylation during acute stress targets enzyme activity, whereas prolonged changes in O-GlcNAcylation during sustained cardiac stress likely result from regulation of enzyme abundance. Consistent with this hypothesis, in a murine model of *in vivo* I/R injury, elevated O-GlcNAcylation was observed following 24 h of reperfusion, and this was associated with increased GFAT1 abundance and increased UDP-GlcNAc levels. The upregulation in GFAT1 and HBP flux was mediated by the

transcription factor Xbp1-spliced that regulates the unfolded protein response (51).

Potential mechanisms underpinning sex-dependent O-GlcNAcylation

Sex and gender disparities have been reported for many human diseases, including CVDs. While hormones play an important role in mediating sex differences, biological sex is determined by both gonadal hormones and sex-specific programs controlled genetically (X and Y chromosomes) (90). The impact of the latter was recently highlighted in a study utilizing the Four Core Genotypes model in which the gene *Sry* is deleted from the Y chromosome and inserted into an autosome resulting in the following four genotypes; XX (ovaries), XX_(Sry+) (testes), XY[–]_(Sry+) (testes), and XY[–] (ovaries). Although these mice develop testes, gonadal sex is uncoupled from the sex chromosome complement. Shi *et al.* (90) identified over 500 proteins that segregate with ovaries/testes and ~150 proteins cosegregating with sex chromosomes in the murine heart. These studies highlighted the glycoprotein A1BG, the abundance of which is elevated in adult and embryonic (prior to gonad formation) female hearts. Loss of A1BG resulted in severely compromised cardiac function only in females (90). Deletion of *Sry* had no impact on the abundance of OGT and OGA in males or females. This finding is consistent with our observations and suggests that regulation of OGT activity is mediated by alternate mechanisms involving the sex chromosomes or through hormone-mediated signaling. Support for the latter comes from reports in skeletal muscle where hormone replacement therapy in postmenopausal women suppressed age-associated upregulation of *Ogt* mRNA and increased *Oga* mRNA levels compared with controls (91). In a separate study in pregnant normotensive and spontaneously hypertensive (primary hypertension model) rats, O-GlcNAcylation was significantly reduced in the thoracic aorta and mesenteric arteries in both groups during pregnancy (92). Estrogen signaling is mediated by the binding of estrogen to the estrogen receptor α , which can then activate multiple signaling pathways that include activation of PI3K/Akt, PKA, mitogen-activated protein kinase, and changes in calcium and NO (93). Notably, OGT is inhibited by nitrosylation. In contrast, denitrosylation of OGT resulted in the upregulation of OGT catalytic activity and increased O-GlcNAcylation (94). However, our observations of elevated O-GlcNAc levels in females are not consistent with enhanced NO in females targeting OGT. Consistent with this observation, OGT was not found in recent screens focused on identifying protein SNO in the heart (6, 95).

To the best of our knowledge, there has been no assessment of the impact of sex or sex hormones (*e.g.*, estrogen) on OGT/OGA abundance, activity, UDP-GlcNAc, and protein O-GlcNAcylation during cardiac I/R injury. We have demonstrated elevated O-GlcNAcylation in female hearts before and after injury that is consistent with the observed elevation in OGT activity in females compared with males. These findings support the hypothesis that the specific activity of OGT is

targeted by biological sex (genetics and sex hormones), thereby impacting cardiac O-GlcNAcylation. Further research including, but not limited to, the assessment of the male and female cardiac O-GlcNAc levels, and regulation of OGT activity by post-translational modifications or protein interactors, would provide more insight into its sex-dependent implications on the cardiovascular system. Such studies will also promote the development of sex-specific therapeutics for the treatment of CVDs. Collectively, these data highlight the importance of studying O-GlcNAc in both males and females and suggest that sex-dependent changes in O-GlcNAcylation could alter disease risk or resilience.

Experimental procedures

Reagents

All chemicals and reagents were of the highest grade and supplied by MilliporeSigma or Thermo Fisher Scientific, unless otherwise indicated.

Antibodies

The following antibodies were used: anti-OGT (O6264; MilliporeSigma, antimouse immunoglobulin M-horseradish peroxidase (HRP) (catalog no.: A8786; MilliporeSigma), anti-mouse IgG-HRP (catalog no.: NA931; Cytiva), anti-rabbit IgG-HRP (catalog no.: NA934; Cytiva); anti-GFAT2 (catalog no.: ab240316; Abcam); anti-heat shock cognate (Hsc) 70 (catalog no.: sc-7298; Santa Cruz Biotechnology); and antichickens IgY-HRP (catalog no.: A30-104p; Fortis Life Sciences). Anti-O-GlcNAc (RL2 and CTD110.6) (96, 97), anti-OGT (AL24) (22) and anti-OGA (345) (98) antibodies were shared by Dr Gerald Hart (CCRC, University of Georgia) and antigen (CTD110.6, AL24, 345) or affinity (RL2) purified prior to use.

Preparation of tissue lysates

The following lysis buffers were used in this study: urea buffer (25 mM Hepes [pH 7.4], 9 M urea), 1% NP-40 buffer (50 mM Tris-Cl [pH 8.0] with 150 mM NaCl and 1% [v/v] Nonidet P-40), or soluble lysis buffer (50 mM Hepes [pH 7.4]) supplemented with the following inhibitors immediately prior to use: protease inhibitor cocktail sets II & III (MilliporeSigma); 10 μ M PUGNAc (A7229, MilliporeSigma); 0.1 mM PMSEF; 0.5 μ M Thiamet G (synthesized by SD ChemMolecules LLC); 10 mM NaF; and 10 mM β -glycerolphosphate. Heart tissue, powdered under liquid nitrogen, was homogenized using a polytron (Cole-Parmer) in the indicated extraction buffer (10 ml/g of heart powder for 1% NP-40 buffer and 20 ml/g of heart powder for urea buffer) for 2 \times 30 s. Tissue debris were pelleted at 18,000g (1% NP-40: 20 min, 4 $^{\circ}$ C; urea: 20 min, 21 $^{\circ}$ C). Protein concentration was assessed using the Pierce 660 nm colorimetric protein assay according to the manufacturer's instructions (Thermo Fisher Scientific).

Electrophoresis and Western blotting

Prior to immunoblotting, samples were desalted and delipidated by methanol-chloroform precipitation and

resuspended in loading buffer at 1.5 mg/ml (99). Equal protein was separated by SDS-PAGE using Bis-Tris (NuPAGE; Thermo Fisher Scientific) polyacrylamide gels. Proteins were electroblotted to nitrocellulose (0.45 μ m, Bio-Rad) and blocked with 3% w/v nonfat milk in 50 mM Tris, pH 7.5, 150 mM NaCl, 0.05% (v/v) Tween-20; 1 h, 21 $^{\circ}$ C. Membranes were incubated with primary antibodies (overnight, 4 $^{\circ}$ C) and subsequently with HRP-conjugated secondary antibodies (1 h, 21 $^{\circ}$ C). Western blots were developed using Immobilon Western chemiluminescent substrate (MilliporeSigma) and captured on a chemiluminescent imaging system (Amersham Biosciences; RGB600 Imager) or using autoradiography film (Amersham Hyperfilm ECL; GE Healthcare). Protein load was assessed by total protein membrane staining (Sypro Ruby [Bio-Rad] or Direct Blue-71 [MilliporeSigma]). Quantitation of Western blots and total protein was performed using Amersham Imager 600 analysis software. A minimum of two biological replicates were assayed in at least four independent experiments. Loading order was changed in independent experiments to avoid positional bias.

OGA activity assays

Assays were performed as previously described (55). Briefly, lysates at equal concentration (1 mg/ml) were desalted into desalting buffer (20 mM Tris, pH 7.8, 20% [v/v] glycerol) using Zeba spin desalting columns (catalog no.: 89808; Thermo Fisher Scientific), and the protein concentration was reassessed (Pierce 660, described previously). The activity of OGA in tissue lysates (10 μ g) was measured in duplicate (technical replicates) in black 96-well plates using 1 mM 4-methylumbelliferyl-GlcNAc (MilliporeSigma) in 50 mM sodium cacodylate, pH 6.4, 0.3% (w/v) bovine serum albumin and 100 mM GalNAc (1 h, 37 $^{\circ}$ C). 100 mM GalNAc is expected to inhibit lysosomal hexosaminidases; however, to rule out contaminating lysosomal hexosaminidase activity, lysates were also assayed in the aforementioned conditions using 1 mM 4-methylumbelliferyl-GalNAc (MilliporeSigma). Assays were quenched with three volumes of glycine, pH 10.75, and the fluorescence intensity was measured using the SpectraMax i3x (Molecular Devices; excitation 368 nm, emission 450 nm). Activity was corrected for protein and expressed as a fold change over the average of male controls. A minimum of two biological replicates were assayed in at least four independent experiments. Loading order was changed in independent experiments to avoid positional bias.

OGT assays

Assays were performed as previously described (55). Briefly, lysates were desalted as described previously (OGA assays). The activity of OGT in tissue lysates (10 μ g) was assessed in triplicate (technical replicates) using 0.5 μ Ci per replicate of [3 H]UDP-GlcNAc (American Radiolabeled Chemicals; specific activity 60 Ci/mmol) and 1 mM casein kinase II acceptor peptide (PGGSTPVSSANMM; The Johns Hopkins University School of Medicine Synthesis and Sequencing Facility) in 50 mM sodium cacodylate, pH 6.4, 0.3% (w/v) bovine serum

Sex differences in O-GlcNAc cycling in the heart

albumin (1 h, 37 °C; 50 µl total assay volume). Assays were quenched with three volumes of 50 mM formate and 500 mM NaCl. Samples were loaded onto a C₁₈ reversed phase 96-well plate (Phenomex; 100 mg resin/well), activated with methanol, and equilibrated in 50 mM formate, 500 mM NaCl. Plates were washed sequentially with 4 ml of 50 mM formate containing 500 mM NaCl, water, and 50 mM formate. The product was eluted from the column with 1 ml of 100% methanol, and the incorporation of radiolabeled GlcNAc was assessed by liquid scintillation counting. Activity was corrected for protein and expressed as a fold change over the average of male controls. A minimum of two biological replicates were assayed in at least four independent experiments. Loading order was changed in independent experiments to avoid positional bias.

Langendorff heart perfusion and treatment protocol

All animal studies were carried out in accordance with the guidelines of the Johns Hopkins Institutional Animal Care and Use Committee under protocol #MO22M213. Male and female C57BL6/J WT mice (Jackson Laboratory) 15 to 21 weeks of age were used in these studies. Mice were anesthetized with I.P. injection of ketamine and xylazine (50 mg/kg) and anticoagulated with 100 µl of heparin (1000 U) administered into the inferior vena cava. Hearts were rapidly excised and placed in ice-cold Krebs–Henseleit (KH) buffer containing 120 mM NaCl, 11 mM D-glucose, 25 mM NaHCO₃, 1.75 mM CaCl₂, 4.7 mM KCl, 1.2 mM MgSO₄, and 1.2 mM KH₂PO₄. The aorta was cannulated and retrogradely perfused under constant pressure of 100 cmH₂O and temperature of 37 °C with oxygenated (95% O₂/5% CO₂) KH buffer. After cannulation, a saran wrap balloon was immediately inserted into the left ventricle to measure HR pressure and HR, LVDP, and HR. Control hearts were perfused for 40 min. For ischemia and I/R hearts, after 20 min of equilibration perfusion, the flow of oxygenated KH buffer through hearts was halted to induce a global normothermic ischemia for 20 min. To induce I/R injury, after 20 min of ischemia, the flow of oxygenated KH buffer was re-established for 120 min of reperfusion. At the end of perfusion, hearts were rapidly frozen in liquid nitrogen and stored in –80 °C. Rate pressure product, the product of LVDP and HR, was calculated and used to measure cardiac contractile function. Only hearts that reached an LVDP of >50 cmH₂O and an HR of >300 bpm were included. LVDP measurements were also used to assess ischemic contracture in ischemic and I/R hearts. Time in contracture was calculated as the time from which LVDP begins to increase during ischemia until the end of the ischemic period. Time in hypercontracture was calculated as the time from which LVDP reaches its maximum value during ischemia until the end of the ischemic period. Duration was calculated as the time between the beginning of contracture and hypercontracture.

Extraction of nucleotide sugars

The following extraction buffer was used to extract nucleotide sugars: methanol:water:chloroform (2:0.8:2) containing

the internal standard UDP-galacturonic acid (25 µM) that is not found in mammals. Hearts were homogenized in extraction buffer using a hard tissue lysing kit (Precellys CK28 Lysing Kit; Bertin Technologies) in a bead-mill tissue homogenizer for 2 × 30 s cycles at 0 °C, 7200 rpm (Precellys Evolution 24; Bertin Instruments). Proteins were pelleted at 18,000g (10 min, 4 °C). Equal amounts of the aqueous layer, which contains the nucleotide sugars, was dried in a SpeedVac. The organic layer was discarded, and the protein pellet was extracted in 50 mM Tris–Cl (pH 7.5), 1% (w/v) SDS, and quantified (bicinchoninic acid protein assay). The remaining protein pellet was hydrolyzed in 0.1 M aqueous NaOH, quantified (bicinchoninic acid protein assay), and the total protein yield was determined. Nucleotide sugars were resuspended in 10 mM ammonium bicarbonate, pH 8.0, and solid-phase cleanup was performed using ENVI-Carb SPE tubes (57109-U, Supelclean; MilliporeSigma) (100). Columns were activated with methanol, followed by 60% (v/v) acetonitrile, 0.3% (v/v) formic acid, and pH 9 (with ammonia). Columns were equilibrated in water prior to the addition of sample and washed with water followed by 60% (v/v) acetonitrile. Nucleotide sugars were eluted using 2 × 0.5 ml 60% (v/v) acetonitrile, 0.3% (v/v) formic acid, and pH 9 (with ammonia). The elution was dried in a SpeedVac. Nucleotide sugars were resuspended in water, filtered through a 0.22 µm hydrophilic polyvinylidene difluoride membrane (UFC30GVNB; MilliporeSigma), and analyzed by high-performance anion exchange chromatography (HPAEC). A minimum of two biological replicates were assayed in at least four independent experiments.

Quantitation of UDP-GlcNAc using HPAEC

Nucleotides and nucleotide sugars (25 µl) were injected onto a Dionex CarboPac column (PA20, 3 × 150 mm; catalog no.: 060142, Thermo Fisher Scientific), equipped with a Dionex CarboPac precolumn (PA20, 3 × 30 mm; catalog no.: 060144, Thermo Fisher Scientific), and analyzed on a Dionex ICS-5000⁺ (Thermo Fisher Scientific) running Chromeleon software (version 7.0; Thermo Scientific). The borate-aided HPAEC separation method was adapted from Oikari *et al.* (101). The column was equilibrated in 120 mM borate (pH 7.5) at 400 µl/min at 60 °C. Nucleotide separation was achieved by introducing 1 M sodium acetate (pH 7.0); a linear gradient of 0 to 32.5% between 0 and 20 min, isocratic conditions between 20 and 45 min at 32.5%; a gradient of 32.5 to 45% between 45 and 51 min, isocratic conditions from 51 to 58 min at 45%; a linear gradient of 40 to 50% between 58 and 60 min; isocratic conditions from 60 to 65 min at 50%; and a linear gradient of 50 to 75% between 65 and 70 min. The column was regenerated in 75% sodium acetate (3 min). Nucleotides were detected at an absorbance of 254 nm. The area under the curve was used to quantify nucleotides per milligram of protein.

Statistical analysis

Graphs and statistical analysis were performed using the GraphPad Prism software (version 9; GraphPad Software, Inc). Data are reported as mean with error bars representing SD.

Biological replicates (N) for each experiment are indicated in the figure legends. A two-way unpaired Student's *t* test was used for the comparison of two groups (Fig. 1). For the comparison of multiple groups or two groups within each treatment, we utilized a one- or two-factor ANOVA as appropriate. An ordinary one-way ANOVA with Tukey's multiple comparison test was performed with all pooled male and female data to compare between multiple groups (Figs. 3–5, S1, and S3). An ordinary two-way ANOVA with Sidak's multiple comparison test was used to compare between males and females within each group (Figs. 2–5 and S3). Pearson correlation coefficients were computed for all correlation analyses (Figs. 4, 5, and S4).

Data availability

A summary of all original data is presented in the article, including all individual data points collected. Unprocessed data are available on request from the corresponding author: Natasha Zachara (nzachara@jhmi.edu).

Supporting information—This article contains supporting information.

Acknowledgments—We thank the Kohr laboratory (Department of Environmental Health and Engineering, Johns Hopkins School of Public Health) for the assistance when using the Langendorff apparatus. We thank Kamau Fahie, PhD, Tiago Januario Da Costa, PhD, Steve Fernandes, MSc, Marissa Martinez, PhD, Cathrine McKen, Fiddia Zahra, MSc, Akanksha Aggarwal, MSc, Kyriakos Papanicolaou, PhD, Olurotimi Olorunfemi Mesubi, MBBS, MPH, Priya Umapathi, MD, Raihan Kabir, ScM, and Michael Fitch, ScM, for the technical help and/or constructive criticism.

Author contributions—B. N. and N. E. Z. conceptualization; B. N., N. E. Z., M. J. K. and N. P. methodology; R. R. and R. H. validation; B. N., R. R., and R. H. formal analysis; B. N., R. R., and R. H. investigation; B. N., R. R., R. H., P. S., M. J. K., and N. E. Z. data curation; B. N. writing—original draft; R. R., R. H., P. S., N. P., M. J. K., and N. E. Z. writing—review & editing

Funding and additional information—This work was supported by the National Institutes of Health grants U01 CA2300978, R01 HL129640, and P01 HL107153 (to N. E. Z.). The content is solely the responsibility of the authors and does not necessarily represent the official views of the National Institutes of Health.

Conflict of interest—The authors declare that they have no conflicts of interest with the contents of this article.

Abbreviations—The abbreviations used are: CVD, cardiovascular disease; GFAT, glutamine-fructose 6 phosphate amidotransferase; GSK3 β , glycogen synthase kinase 3 β ; HBP, hexosamine biosynthetic pathway; HPAEC, high-performance anion exchange chromatography; HR, heart rate; HRP, horseradish peroxidase; IgG, immunoglobulin G; IPC, ischemic preconditioning; I/R, ischemia-reperfusion; KH, Krebs–Henseleit buffer; LVDP, left ventricular developed pressure; MI, myocardial infarction; NO, nitric oxide; OGA, O-GlcNAcase; OGT, O-GlcNAc transferase; O-GlcNAc, O-linked β -GlcNAc; rIPC, remote ischemic preconditioning; SNO,

S-nitrosylation; TAC, transverse aortic constriction; Xb1, X-box binding protein 1.

References

- Reue, K., and Wiese, C. B. (2022) Illuminating the mechanisms underlying sex differences in cardiovascular disease. *Circ. Res.* **130**, 1747–1762
- Tsao, C. W., Aday, A. W., Almarazgo, Z. I., Anderson, C. A. M., Arora, P., Avery, C. L., *et al.* (2023) Heart disease and stroke statistics—2023 update: a report from the American heart association. *Circulation* **147**, e93–e621
- Mosca, L., Barrett-Connor, E., and Wenger, N. K. (2011) Sex/gender differences in cardiovascular disease prevention. *Circulation* **124**, 2145–2154
- Peters, H. W., Westendorp, I. C. D., Hak, A. E., Grobbee, D. E., Stehouwer, C. D. A., Hofman, A., *et al.* (1999) Menopausal status and risk factors for cardiovascular disease. *J. Intern. Med.* **246**, 521–528
- Cagnacci, A., Cannoletta, M., Palma, F., Zanin, R., Xholli, A., and Volpe, A. (2012) Menopausal symptoms and risk factors for cardiovascular disease in postmenopause. *Climacteric* **15**, 157–162
- Shao, Q., Fallica, J., Casin, K. M., Murphy, E., Steenbergen, C., and Kohr, M. J. (2016) Characterization of the sex-dependent myocardial S-nitrosothiol proteome. *Am. J. Physiol. Heart Circ. Physiol.* **310**, H505–H515
- Sun, J., Picht, E., Ginsburg, K. S., Bers, D. M., Steenbergen, C., and Murphy, E. (2006) Hypercontractile female hearts exhibit increased S-nitrosylation of the L-type Ca²⁺ channel α 1 subunit and reduced ischemia/reperfusion injury. *Circ. Res.* **98**, 403–411
- Lagranha, C. J., Deschamps, A., Aponte, A., Steenbergen, C., and Murphy, E. (2010) Sex differences in the phosphorylation of mitochondrial proteins result in reduced production of reactive oxygen species and cardioprotection in females. *Circ. Res.* **106**, 1681–1691
- Lin, J., Steenbergen, C., Murphy, E., and Sun, J. (2009) Estrogen receptor- β activation results in S-nitrosylation of proteins involved in cardioprotection. *Circulation* **120**, 245–254
- Hale, S. L., Birnbaum, Y., and Kloner, R. A. (1996) β -Estradiol, but not α -estradiol, reduces myocardial necrosis in rabbits after ischemia and reperfusion. *Am. Heart J.* **132**, 258–262
- Booth, E. A., Obeid, N. R., and Lucchesi, B. R. (2005) Activation of estrogen receptor- α protects the *in vivo* rabbit heart from ischemia-reperfusion injury. *Am. J. Physiol. Heart Circ. Physiol.* **289**, H2039–H2047
- Dubey, R. K., Imthurn, B., Zacharia, L. C., and Jackson, E. K. (2004) Hormone replacement therapy and cardiovascular disease. *Hypertension* **44**, 789–795
- Casin, K. M., Fallica, J., Mackowski, N., Veenema, R. J., Chan, A., St Paul, A., *et al.* (2018) S-nitrosoglutathione reductase is essential for protecting the female heart from ischemia-reperfusion injury. *Circ. Res.* **123**, 1232–1243
- Hart, G. W. (2019) Nutrient regulation of signaling and transcription. *J. Biol. Chem.* **294**, 2211–2231
- Zachara, N. E. (2018) Critical observations that shaped our understanding of the function(s) of intracellular glycosylation (O-GlcNAc). *FEBS Lett.* **592**, 3950–3975
- Wulff-Fuentes, E., Berendt, R. R., Massman, L., Danner, L., Malard, F., Vora, J., *et al.* (2021) The human O-GlcNAc database and meta-analysis. *Sci. Data* **8**, 25
- Rao, X., Duan, X., Mao, W., Li, X., Li, Z., Li, Q., *et al.* (2015) O-GlcNAcylation of G6PD promotes the pentose phosphate pathway and tumor growth. *Nat. Commun.* **6**, 8468
- Yuzwa, S. A., Shan, X., Macauley, M. S., Clark, T., Skorobogatko, Y., Vosseller, K., *et al.* (2012) Increasing O-GlcNAc slows neurodegeneration and stabilizes tau against aggregation. *Nat. Chem. Biol.* **8**, 393–399
- Yi, W., Clark, P. M., Mason, D. E., Keenan, M. C., Hill, C., Goddard, W. A., *et al.* (2012) Phosphofructokinase 1 glycosylation regulates cell growth and metabolism. *Science* **337**, 975–980

Sex differences in O-GlcNAc cycling in the heart

20. Konzman, D., Abramowitz, L. K., Steenackers, A., Mukherjee, M. M., Na, H.-J., and Hanover, J. A. (2020) O-GlcNAc: regulator of signaling and epigenetics linked to X-linked intellectual disability. *Front. Genet.* **11**, 605263
21. Lewis, B. A., and Hanover, J. A. (2014) O-GlcNAc and the epigenetic regulation of gene expression. *J. Biol. Chem.* **289**, 34440–34448
22. Kreppel, L. K., Blomberg, M. A., and Hart, G. W. (1997) Dynamic glycosylation of nuclear and cytosolic proteins cloning and characterization of A unique O-GlcNAc transferase with multiple tetrapeptide repeats. *J. Biol. Chem.* **272**, 9308–9315
23. Lubas, W. A., Frank, D. W., Krause, M., and Hanover, J. A. (1997) O-linked GlcNAc transferase is a conserved nucleocytoplasmic protein containing tetrapeptide repeats. *J. Biol. Chem.* **272**, 9316–9324
24. Gao, Y., Wells, L., Comer, F. I., Parker, G. J., and Hart, G. W. (2001) Dynamic O-glycosylation of nuclear and cytosolic proteins cloning and characterization of A neutral, cytosolic β -N-acetylglucosaminidase from human brain. *J. Biol. Chem.* **276**, 9838–9845
25. O'Donnell, N., Zachara, N. E., Hart, G. W., and Marth, J. D. (2004) Ogt-dependent X-chromosome-linked protein glycosylation is a requisite modification in somatic cell function and embryo viability. *Mol. Cell Biol.* **24**, 1680–1690
26. Yang, Y. R., Song, M., Lee, H., Jeon, Y., Choi, E., Jang, H., *et al.* (2012) O-GlcNAcase is essential for embryonic development and maintenance of genomic stability. *Aging Cell* **11**, 439–448
27. Shafi, R., Iyer, S. P. N., Ellies, L. G., O'Donnell, N., Marek, K. W., Chui, D., *et al.* (2000) The O-GlcNAc transferase gene resides on the X chromosome and is essential for embryonic stem cell viability and mouse ontogeny. *Proc. Natl. Acad. Sci. U. S. A.* **97**, 5735–5739
28. Zachara, N. E., O'Donnell, N., Cheung, W. D., Mercer, J. J., Marth, J. D., and Hart, G. W. (2004) Dynamic O-GlcNAc modification of nucleocytoplasmic proteins in response to stress A survival response of mammalian cells. *J. Biol. Chem.* **279**, 30133–30142
29. Kazemi, Z., Chang, H., Haserodt, S., McKen, C., and Zachara, N. E. (2010) O-linked β -N-acetylglucosamine (O-GlcNAc) regulates stress-induced heat shock protein expression in a GSK-3 β -dependent manner. *J. Biol. Chem.* **285**, 39096–39107
30. Martinez, M. R., Dias, T. B., Natov, P. S., and Zachara, N. E. (2017) Stress-induced O-GlcNAcylation: an adaptive process of injured cells. *Biochem. Soc. Trans* **45**, 237–249
31. Groves, J. A., Lee, A., Yildirim, G., and Zachara, N. E. (2013) Dynamic O-GlcNAcylation and its roles in the cellular stress response and homeostasis. *Cell Stress Chaperones* **18**, 535–558
32. Jensen, R. V., Johnsen, J., Kristiansen, S. B., Zachara, N. E., and Bøtker, H. E. (2013) Ischemic preconditioning increases myocardial O-GlcNAc glycosylation. *Scand. Cardiovasc. J.* **47**, 168–174
33. Jensen, R. V., Zachara, N. E., Nielsen, P. H., Kimose, H. H., Kristiansen, S. B., and Bøtker, H. E. (2013) Impact of O-GlcNAc on cardioprotection by remote ischaemic preconditioning in non-diabetic and diabetic patients. *Cardiovasc. Res.* **97**, 369–378
34. Fülöp, N., Zhang, Z., Marchase, R. B., and Chatham, J. C. (2007) Glucosamine cardioprotection in perfused rat hearts associated with increased O-linked N-acetylglucosamine protein modification and altered p38 activation. *Am. J. Physiol. Heart Circ. Physiol.* **292**, H2227–H2236
35. Liu, J., Pang, Y., Chang, T., Bounelis, P., Chatham, J. C., and Marchase, R. B. (2006) Increased hexosamine biosynthesis and protein O-GlcNAc levels associated with myocardial protection against calcium paradox and ischemia. *J. Mol. Cell Cardiol.* **40**, 303–312
36. Liu, J., Marchase, R. B., and Chatham, J. C. (2007) Increased O-GlcNAc levels during reperfusion lead to improved functional recovery and reduced calpain proteolysis. *Am. J. Physiol. Heart Circ. Physiol.* **293**, H1391–H1399
37. Jones, S. P., Zachara, N. E., Ngoh, G. A., Hill, B. G., Teshima, Y., Bhatnagar, A., *et al.* (2008) Cardioprotection by N-acetylglucosamine linkage to cellular proteins. *Circulation* **117**, 1172–1182
38. Champattanachai, V., Marchase, R. B., and Chatham, J. C. (2007) Glucosamine protects neonatal cardiomyocytes from ischemia-reperfusion injury via increased protein-associated O-GlcNAc. *Am. J. Physiol. Cell Physiol.* **292**, C178–C187
39. Laczay, B., Marsh, S. A., Brocks, C. A., Wittmann, I., and Chatham, J. C. (2010) Inhibition of O-GlcNAcase in perfused rat hearts by NAG-thiazolines at the time of reperfusion is cardioprotective in an O-GlcNAc-dependent manner. *Am. J. Physiol. Heart Circ. Physiol.* **299**, H1715–H1727
40. Dassanayaka, S., and Jones, S. P. (2014) O-GlcNAc and the cardiovascular system. *Pharmacol. Therapeut.* **142**, 62–71
41. Ngoh, G. A., Facundo, H. T., Zafir, A., and Jones, S. P. (2010) O-GlcNAc signaling in the cardiovascular system. *Circ. Res.* **107**, 171–185
42. Ngoh, G. A., Hamid, T., Prabhu, S. D., and Jones, S. P. (2009) O-GlcNAc signaling attenuates ER stress-induced cardiomyocyte death. *Am. J. Physiol. Heart Circ. Physiol.* **297**, H1711–H1719
43. Jensen, R. V., Andreadou, I., Hausenloy, D. J., and Bøtker, H. E. (2019) The role of O-GlcNAcylation for protection against ischemia-reperfusion injury. *Int. J. Mol. Sci.* **20**, 404
44. Watson, L. J., Facundo, H. T., Ngoh, G. A., Ameen, M., Brainard, R. E., Lemma, K. M., *et al.* (2010) O-linked β -N-acetylglucosamine transferase is indispensable in the failing heart. *Proc. Natl. Acad. Sci. U. S. A.* **107**, 17797–17802
45. Ngoh, G. A., Facundo, H. T., Hamid, T., Dillmann, W., Zachara, N. E., and Jones, S. P. (2009) Unique hexosaminidase reduces metabolic survival signal and sensitizes cardiac myocytes to hypoxia/reoxygenation injury. *Circ. Res.* **104**, 41–49
46. Ngoh, G. A., Watson, L. J., Facundo, H. T., and Jones, S. P. (2011) Augmented O-GlcNAc signaling attenuates oxidative stress and calcium overload in cardiomyocytes. *Amino Acids* **40**, 895–911
47. Ngoh, G. A., Watson, L. J., Facundo, H. T., Dillmann, W., and Jones, S. P. (2008) Non-canonical glycosyltransferase modulates post-hypoxic cardiac myocyte death and mitochondrial permeability transition. *J. Mol. Cell Cardiol.* **45**, 313–325
48. Zhu, W. Z., Ledee, D., and Olson, A. K. (2021) Temporal regulation of protein O-GlcNAc levels during pressure-overload cardiac hypertrophy. *Physiol. Rep.* **9**, e14965
49. Howerton, C. L., Morgan, C. P., Fischer, D. B., and Bale, T. L. (2013) O-GlcNAc transferase (OGT) as a placental biomarker of maternal stress and reprogramming of CNS gene transcription in development. *Proc. Natl. Acad. Sci. U. S. A.* **110**, 5169–5174
50. Narayanan, B., Zahra, F., Reeves, R. A., Aggarwal, A., O'Meally, R. N., Henry, R., *et al.* (2023) Differential Detection of O-GlcNAcylated proteins in the heart using antibodies. *Anal. Biochem.* **678**, 115262
51. Wang, Z. V., Deng, Y., Gao, N., Pedrozo, Z., Li, D. L., Morales, C. R., *et al.* (2014) Spliced X-box binding protein 1 couples the unfolded protein response to hexosamine biosynthetic pathway. *Cell* **156**, 1179–1192
52. Reichelt, M. E., Mellor, K. M., Curl, C. L., Stapleton, D., and Delbridge, L. M. D. (2013) Myocardial glycophagy — a specific glycogen handling response to metabolic stress is accentuated in the female heart. *J. Mol. Cell Cardiol.* **65**, 67–75
53. Martinez, M., Renuse, S., Kreimer, S., O'Meally, R., Natov, P., Madugundu, A. K., *et al.* (2021) Quantitative proteomics reveals that the OGT interactome is remodeled in response to oxidative stress. *Mol. Cell Proteomics* **20**, 100069
54. Groves, J. A., Maduka, A. O., O'Meally, R. N., Cole, R. N., and Zachara, N. E. (2017) Fatty acid synthase inhibits the O-GlcNAcase during oxidative stress. *J. Biol. Chem.* **292**, 6493–6511
55. Fahie, K., Narayanan, B., Zahra, F., Reeves, R., Fernandes, S. M., Hart, G. W., *et al.* (2021) Detection and analysis of proteins modified by O-linked N-acetylglucosamine. *Curr. Protoc. I.* **1**, e129
56. Sengupta, S., Sharma, C. G. N., and Jordan, V. C. (2010) Estrogen regulation of X-box binding protein-1 and its role in estrogen induced growth of breast and endometrial cancer cells. *Horm. Mol. Biol. Clin. Invest.* **2**, 235–243
57. Olson, A. K., Bouchard, B., Zhu, W. Z., Chatham, J. C., and Rosiers, C. D. (2020) First characterization of glucose flux through the hexosamine biosynthesis pathway (HBP) in *ex vivo* mouse heart. *J. Biol. Chem.* **295**, 2018–2033

58. Lunde, I. G., Aronsen, J. M., Kvaløy, H., Qvigstad, E., Sjaastad, I., Tønnessen, T., *et al.* (2012) Cardiac O-GlcNAc signaling is increased in hypertrophy and heart failure. *Physiol. Genomics* **44**, 162–172
59. Lima, V. V., Giachini, F. R., Hardy, D. M., Webb, R. C., and Tostes, R. C. (2011) O-GlcNAcylation: a novel pathway contributing to the effects of endothelin in the vasculature. *Am. J. Physiol. Regul. Integr. Comp. Physiol.* **300**, R236–R250
60. Erickson, J. R., Pereira, L., Wang, L., Han, G., Ferguson, A., Dao, K., *et al.* (2013) Diabetic hyperglycaemia activates CaMKII and arrhythmias by O-linked glycosylation. *Nature* **502**, 372–376
61. Champattanachai, V., Marchase, R. B., and Chatham, J. C. (2008) Glucosamine protects neonatal cardiomyocytes from ischemia-reperfusion injury *via* increased protein O-GlcNAc and increased mitochondrial Bcl-2. *Am. J. Physiol. Cell Physiol.* **294**, C1509–C1520
62. Huynh, V. N., Benavides, G. A., Johnson, M. S., Ouyang, X., Chacko, B. K., Osuma, E., *et al.* (2022) Acute inhibition of OGA sex-dependently alters the networks associated with bioenergetics, autophagy, and neurodegeneration. *Mol. Brain* **15**, 22
63. Tan, Z.-W., Fei, G., Paulo, J. A., Bellaousov, S., Martin, S. E. S., Duveau, D. Y., *et al.* (2020) O-GlcNAc regulates gene expression by controlling detained intron splicing. *Nucleic Acids Res.* **48**, 5656–5669
64. Davies, M. P. A., Barraclough, D. L., Stewart, C., Joyce, K. A., Eccles, R. M., Barraclough, R., *et al.* (2008) Expression and splicing of the unfolded protein response gene XBP-1 are significantly associated with clinical outcome of endocrine-treated breast cancer. *Int. J. Cancer* **123**, 85–88
65. Akella, N. M., Ciraku, L., and Reginato, M. J. (2019) Fueling the fire: emerging role of the hexosamine biosynthetic pathway in cancer. *BMC Biol.* **17**, 52
66. Taparra, K., Wang, H., Malek, R., Lafargue, A., Barbhuiya, M. A., Wang, X., *et al.* (2018) O-GlcNAcylation is required for mutant KRAS-induced lung tumorigenesis. *J. Clin. Invest.* **128**, 4924–4937
67. Muha, V., Authier, F., Szoke-Kovacs, Z., Johnson, S., Gallagher, J., McNeilly, A., *et al.* (2021) Loss of O-GlcNAcase catalytic activity leads to defects in mouse embryogenesis. *J. Biol. Chem.* **296**, 100439
68. McClain, D. A., Lubas, W. A., Cooksey, R. C., Hazel, M., Parker, G. J., Love, D. C., *et al.* (2002) Altered glycan-dependent signaling induces insulin resistance and hyperleptinemia. *Proc. Natl. Acad. Sci. U. S. A.* **99**, 10695–10699
69. Prakoso, D., Lim, S. Y., Erickson, J. R., Wallace, R. S., Lees, J. G., Tate, M., *et al.* (2021) Fine-tuning the cardiac O-GlcNAcylation regulatory enzymes governs the functional and structural phenotype of the diabetic heart. *Cardiovasc. Res.* **118**, cvab043
70. Dassanayaka, S., Brainard, R. E., Watson, L. J., Long, B. W., Brittan, K. R., DeMartino, A. M., *et al.* (2017) Cardiomyocyte Ogt limits ventricular dysfunction in mice following pressure overload without affecting hypertrophy. *Basic Res. Cardiol.* **112**, 23
71. Penna, C., Tullio, F., Merlino, A., Moro, F., Raimondo, S., Rastaldo, R., *et al.* (2009) Postconditioning cardioprotection against infarct size and post-ischemic systolic dysfunction is influenced by gender. *Basic Res. Cardiol.* **104**, 390–402
72. Hardie, D. G. (2018) Keeping the home fires burning†: AMP-activated protein kinase. *J. Roy. Soc. Interf.* **15**, 20170774
73. Bullen, J. W., Balsbaugh, J. L., Chanda, D., Shabanowitz, J., Hunt, D. F., Neumann, D., *et al.* (2014) Cross-talk between two essential nutrient-sensitive enzymes O-GlcNAc transferase (OGT) and AMP-ACTIVATED protein kinase. *J. Biol. Chem.* **289**, 10592–10606
74. Kaasik, K., Kivimäe, S., Allen, J. J., Chalkley, R. J., Huang, Y., Baer, K., *et al.* (2013) Glucose sensor O-GlcNAcylation coordinates with phosphorylation to regulate circadian clock. *Cell Metab.* **17**, 291–302
75. Chang, Q., Su, K., Baker, J. R., Yang, X., Paterson, A. J., and Kudlow, J. E. (2000) Phosphorylation of human glutamine:fructose-6-phosphate amidotransferase by cAMP-dependent protein kinase at serine 205 blocks the enzyme activity. *J. Biol. Chem.* **275**, 21981–21987
76. Tong, H., Imahashi, K., Steenbergen, C., and Murphy, E. (2002) Phosphorylation of glycogen synthase kinase-3 β during preconditioning through a phosphatidylinositol-3-kinase-dependent pathway is cardioprotective. *Circ. Res.* **90**, 377–379
77. Zhai, P., and Sadoshima, J. (2008) Overcoming an energy crisis? *Circ. Res.* **103**, 910–913
78. Haushalter, K. J., Schilling, J. M., Song, Y., Sastri, M., Perkins, G. A., Strack, S., *et al.* (2019) Cardiac ischemia-reperfusion injury induces ROS-dependent loss of PKA regulatory subunit RI α . *Am. J. Physiol. Heart Circ. Physiol.* **317**, H1231–H1242
79. Ishikita, A., Matsushima, S., Ikeda, S., Okabe, K., Nishimura, R., Tado-koro, T., *et al.* (2021) GFAT2 mediates cardiac hypertrophy through HBP-O-GlcNAcylation-Akt pathway. *Iscience* **24**, 103517
80. Dassanayaka, S., Brittan, K. R., Long, B. W., Higgins, L. A., Bradley, J. A., Audam, T. N., *et al.* (2020) Cardiomyocyte Oga haploinsufficiency increases O-GlcNAcylation but hastens ventricular dysfunction following myocardial infarction. *PLoS One* **15**, e0242250
81. Watson, L. J., Long, B. W., DeMartino, A. M., Brittan, K. R., Readnower, R. D., Brainard, R. E., *et al.* (2014) Cardiomyocyte Ogt is essential for postnatal viability. *Am. J. Physiol. Heart Circ. Physiol.* **306**, H142–H153
82. Umaphathi, P., Banerjee, P. S., Zachara, N. E., Abrol, N., Wang, Q., Mesubi, O. O., *et al.* (2021) Excessive O - GlcNAcylation causes heart failure and sudden death. *Circulation*. <https://doi.org/10.1161/circulationaha.120.051911>
83. Tran, D. H., May, H. L., Li, Q., Luo, X., Huang, J., Zhang, G., *et al.* (2020) Chronic activation of hexosamine biosynthesis in the heart triggers pathological cardiac remodeling. *Nat. Commun.* **11**, 1771
84. Mesubi, O. O., Rokita, A. G., Abrol, N., Wu, Y., Chen, B., Wang, Q., *et al.* (2020) Oxidized-CaMKII and O-GlcNAcylation cause increased atrial fibrillation in diabetic mice by distinct mechanisms. *J. Clin. Invest.* <https://doi.org/10.1172/jci95747>
85. Nagy, T., Champattanachai, V., Marchase, R. B., and Chatham, J. C. (2006) Glucosamine inhibits angiotensin II-induced cytoplasmic Ca²⁺ elevation in neonatal cardiomyocytes *via* protein-associated O-linked N-acetylglucosamine. *Am. J. Physiol. Cell Physiol.* **290**, C57–C65
86. Zou, L., Yang, S., Hu, S., Chaudry, I. H., Marchase, R. B., and Chatham, J. C. (2007) The protective effects of pugnac on cardiac function after TRAUMA-HEMORRHAGE are mediated *via* increased protein O-GlcNAc levels. *Shock* **27**, 402–408
87. Zou, L., Yang, S., Champattanachai, V., Hu, S., Chaudry, I. H., Marchase, R. B., *et al.* (2009) Glucosamine improves cardiac function following trauma-hemorrhage by increased protein O-GlcNAcylation and attenuation of NF- κ B signaling. *Am. J. Physiol. Heart Circ. Physiol.* **296**, H515–H523
88. Facundo, H. T., Brainard, R. E., Watson, L. J., Ngoh, G. A., Hamid, T., Prabhu, S. D., *et al.* (2012) O-GlcNAc signaling is essential for NFAT-mediated transcriptional reprogramming during cardiomyocyte hypertrophy. *Am. J. Physiol. Heart Circ. Physiol.* **302**, H2122–H2130
89. Muthusamy, S., DeMartino, A. M., Watson, L. J., Brittan, K. R., Zafir, A., Dassanayaka, S., *et al.* (2014) MicroRNA-539 is up-regulated in failing heart, and suppresses O-GlcNAcase expression. *J. Biol. Chem.* **289**, 29665–29676
90. Shi, W., Sheng, X., Dorr, K. M., Hutton, J. E., Emerson, J. I., Davies, H. A., *et al.* (2021) Cardiac proteomics reveals sex chromosome-dependent differences between males and females that arise prior to gonad formation. *Dev. Cell* **56**, 3019–3034.e7
91. Toivonen, M. H. M., Pöllänen, E., Ahtiainen, M., Suominen, H., Taaffe, D. R., Cheng, S., *et al.* (2013) OGT and OGA expression in postmenopausal skeletal muscle associates with hormone replacement therapy and muscle cross-sectional area. *Exp. Gerontol.* **48**, 1501–1504
92. Troiano, J. A., Potje, S. R., Graton, M. E., Silva, D. S., da Costa, R. M., Tostes, R. C., *et al.* (2021) Pregnancy decreases O-GlcNAc-modified proteins in systemic arteries of normotensive and spontaneously hypertensive rats. *Life Sci.* **266**, 118885
93. da Silva, J. S., Montagnoli, T. L., Rocha, B. S., Tacco, M. L. C. A., Marinho, S. C. P., and Zapata-Sudo, G. (2021) Estrogen receptors: therapeutic perspectives for the treatment of cardiac dysfunction after myocardial infarction. *Int. J. Mol. Sci.* **22**, 525

Sex differences in O-GlcNAc cycling in the heart

94. Ryu, I.-H., and Do, S.-I. (2011) Denitrosylation of S-nitrosylated OGT is triggered in LPS-stimulated innate immune response. *Biochem. Biophys. Res. Commun.* **408**, 52–57
95. Lau, B., Fazelinia, H., Mohanty, I., Raimo, S., Tenopoulou, M., Doulias, P.-T., *et al.* (2021) Endogenous S-nitrosocysteine proteomic inventories identify a core of proteins in heart metabolic pathways. *Redox Biol.* **47**, 102153
96. Snow, C. M., Senior, A., and Gerace, L. (1987) Monoclonal antibodies identify a group of nuclear pore complex glycoproteins. *J. Cell Biol.* **104**, 1143–1156
97. Comer, F. I., Vosseller, K., Wells, L., Accavitti, M. A., and Hart, G. W. (2001) Characterization of a mouse monoclonal antibody specific for O-linked N-acetylglucosamine. *Anal. Biochem.* **293**, 169–177
98. Butkinaree, C., Cheung, W. D., Park, S., Park, K., Barber, M., and Hart, G. W. (2008) Characterization of β -N-acetylglucosaminidase cleavage by caspase-3 during apoptosis. *J. Biol. Chem.* **283**, 23557–23566
99. Lee, A., Miller, D., Henry, R., Paruchuri, V. D. P., O'Meally, R. N., Boronina, T., *et al.* (2016) Combined antibody/lectin enrichment identifies extensive changes in the O-GlcNAc sub-proteome upon oxidative stress. *J. Proteome Res.* **15**, 4318–4336
100. Behmüller, R., Forstenlehner, I. C., Tenhaken, R., and Huber, C. G. (2014) Quantitative HPLC-MS analysis of nucleotide sugars in plant cells following off-line SPE sample preparation. *Anal. Bioanal. Chem.* **406**, 3229–3237
101. Oikari, S., Venäläinen, T., and Tammi, M. (2014) Borate-aided anion exchange high-performance liquid chromatography of uridine diphosphate-sugars in brain, heart, adipose and liver tissues. *J. Chromatogr. A.* **1323**, 82–86